Supplement of Atmos. Chem. Phys., 22, 9461–9482, 2022
https://doi.org/10.5194/acp-22-9461-2022-supplement

Atmospheric Chemistry and Physics
Open Access
EGU

Supplement of

Iron (Fe) speciation in size-fractionated aerosol particles in the Pacific Ocean: The role of organic complexation of Fe with humic-like substances in controlling Fe solubility

Kohei Sakata et al.

Correspondence to: Kohei Sakata (sakata.kohei@nies.go.jp)

Supplemental Figures

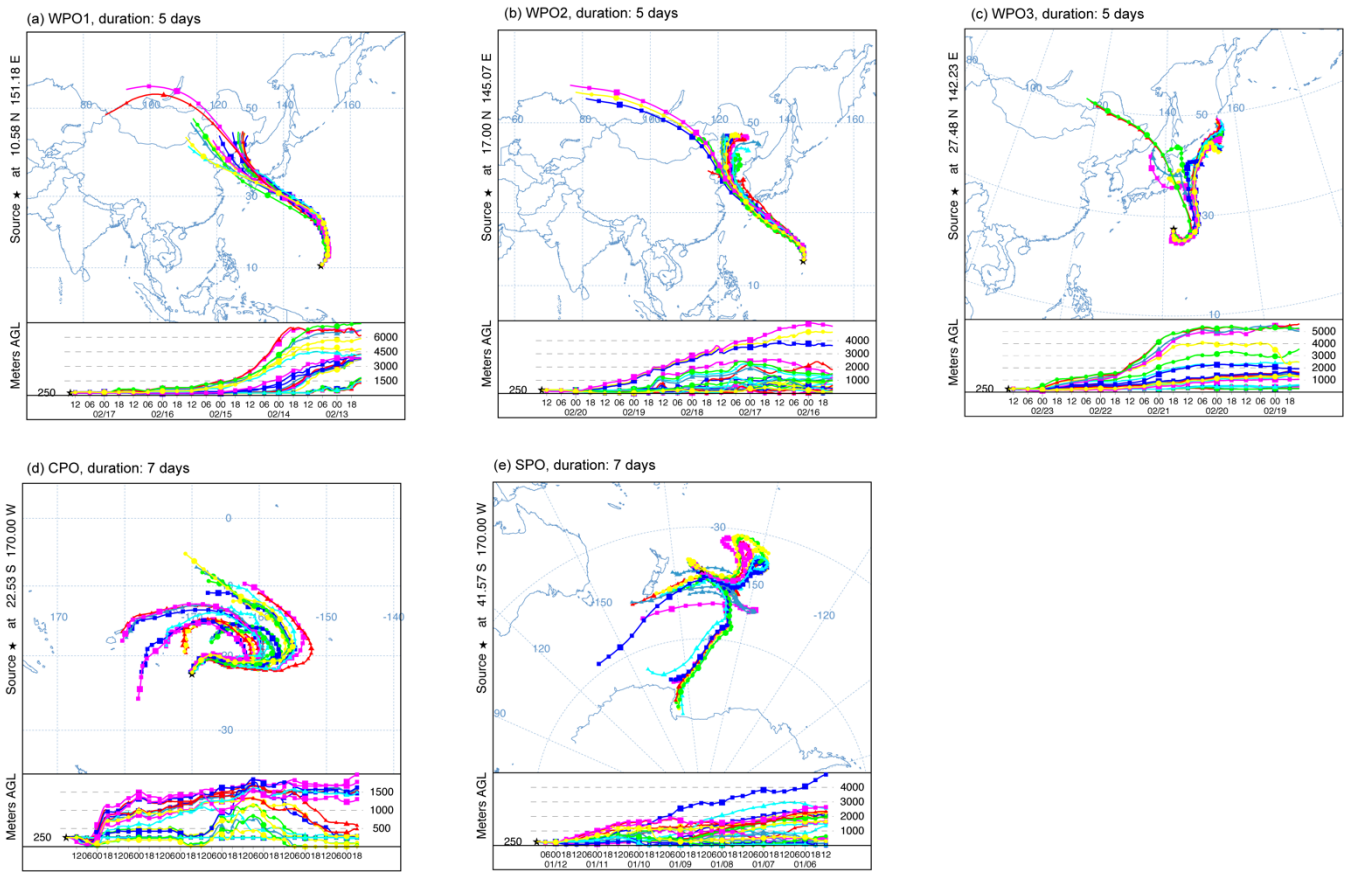

Figure S1: Backward trajectories of (a) WPO1, (b) WPO2, (c) WPO3, (d) CPO, and (e) SPO obtained by the ensemble mode (Stein et al., 2015). The backward trajectories were calculated at midpoint of each sampling region shown in Fig. S1. Duration of WPO1 to WPO3 were 5 days, where those for CPO and SPO samples were 7 days.

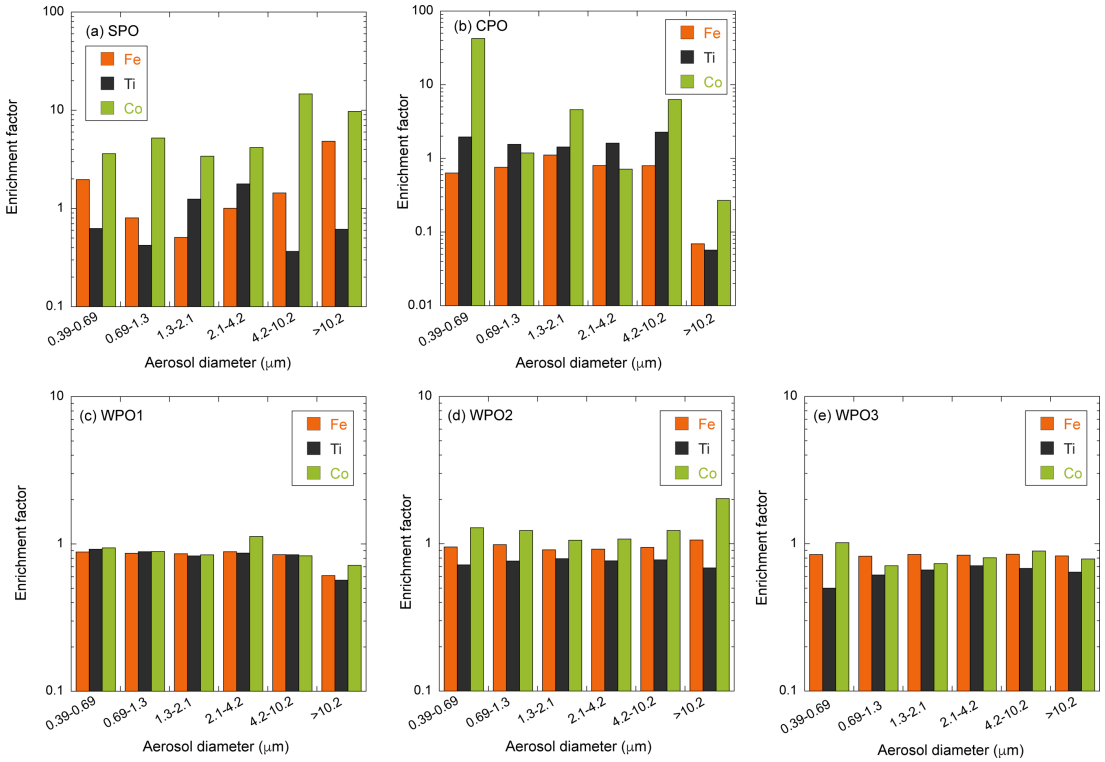

Figure S2: Enrichment factors of Fe, Ti, and Co in size-fractionated marine aerosol particles collected in (a) SPO, (b) CPO, (c) WPO1, (d) WPO2, and (e) WPO3.

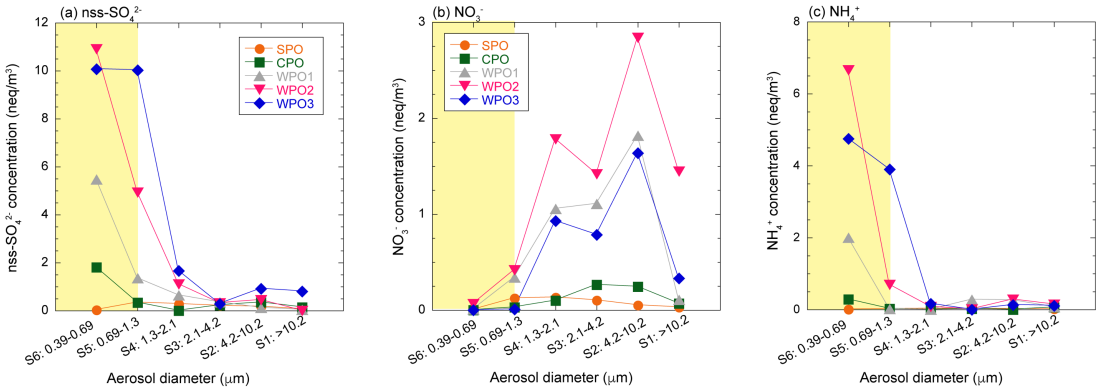

Figure S3: Size-distributions of (a) nss-SO_4^{2-}, (b) NO_3^-, and (c) NH_4^+ concentrations.

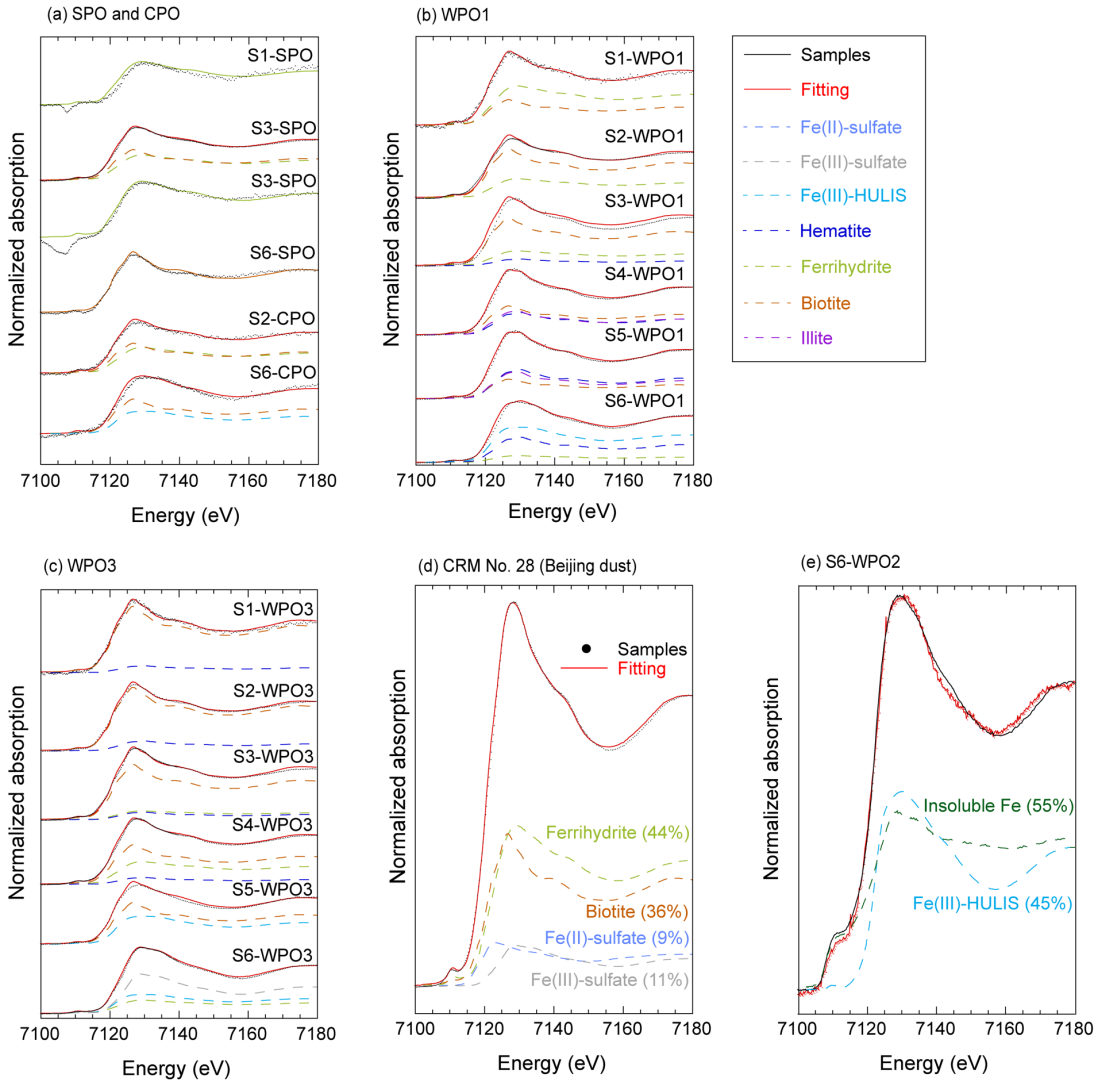

Figure S4: Fe K-edge XANES spectra of size-fractionated aerosols in (a) CPO and SPO, (b) WPO1, (c) WPO3, (d) CRM No. 28, and (e) S6-WPO2. XANES spectra and LCF results are represented by black and red lines, respectively. The XANES spectrum of insoluble Fe in panel (e) was obtained by residue of water-extraction of L-Fe. The percentages in parentheses in panels (d) and (e) are shown relative abundance of fitting species.

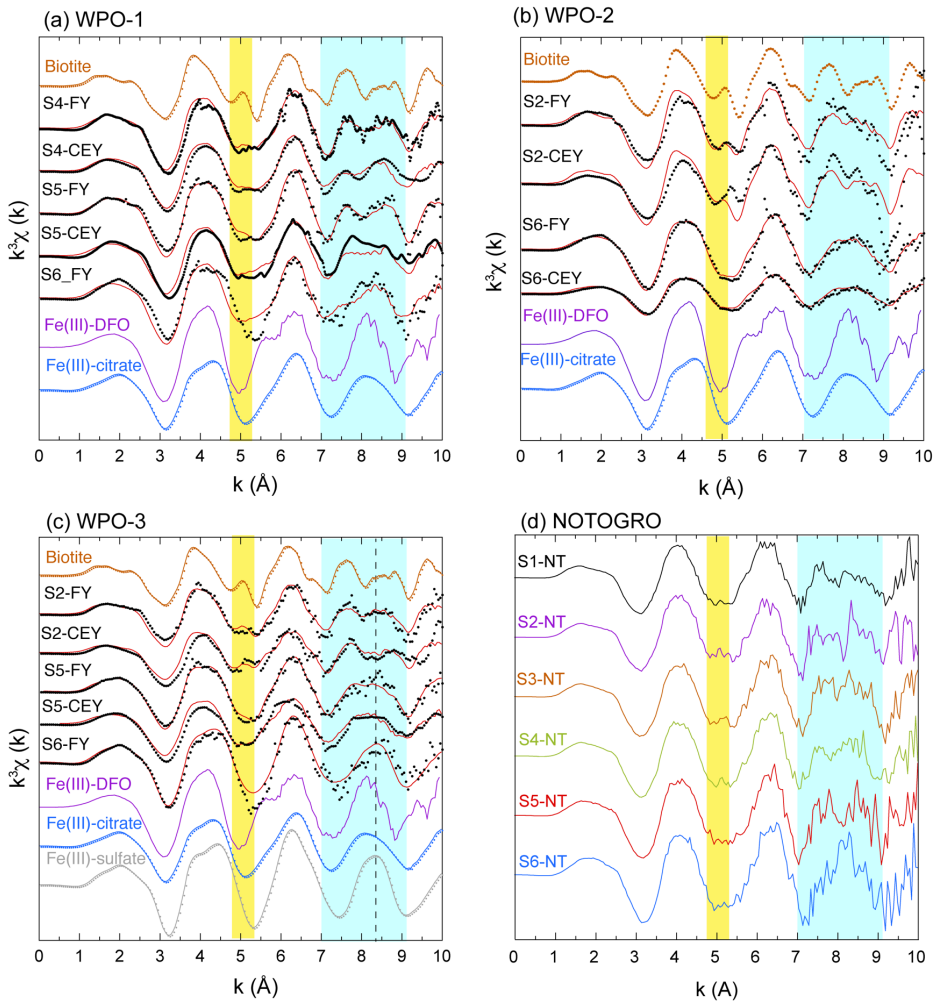

Figure S5: Iron K-edge EXAFS spectra of aerosol particles collected in (a) WPO1, (b) WPO2, (c) WPO3, and (d) NOTOGRO. FY and CEY in panels b and c implied fluorescence yield (FY: bulk sensitive speciation) and conversion electron yield (CEY: surface sensitive speciation), respectively. Yellow shaded region: small peak associated with biotite could be found in EXAFS spectra of coarse aerosol particles, whereas EXAFS spectra of fine aerosol particles did not have the small peak. Light blue region: EXAFS spectra of $PM_{>1.3}$ clearly reflected two peaks of biotite, whereas those of $PM_{1.3}$ have a single peak in the same region. The features of EXAFS spectra of $PM_{1.3}$ in both yellow and light blue regions were similar to those of Fe(III)-HULIS. Dashed line in panel (c) shows peak position of Fe(III)-sulfate. The peak position of S6-FY in WPO3 were similar to Fe(III)-sulfate rather than Fe(III)-HULIS.

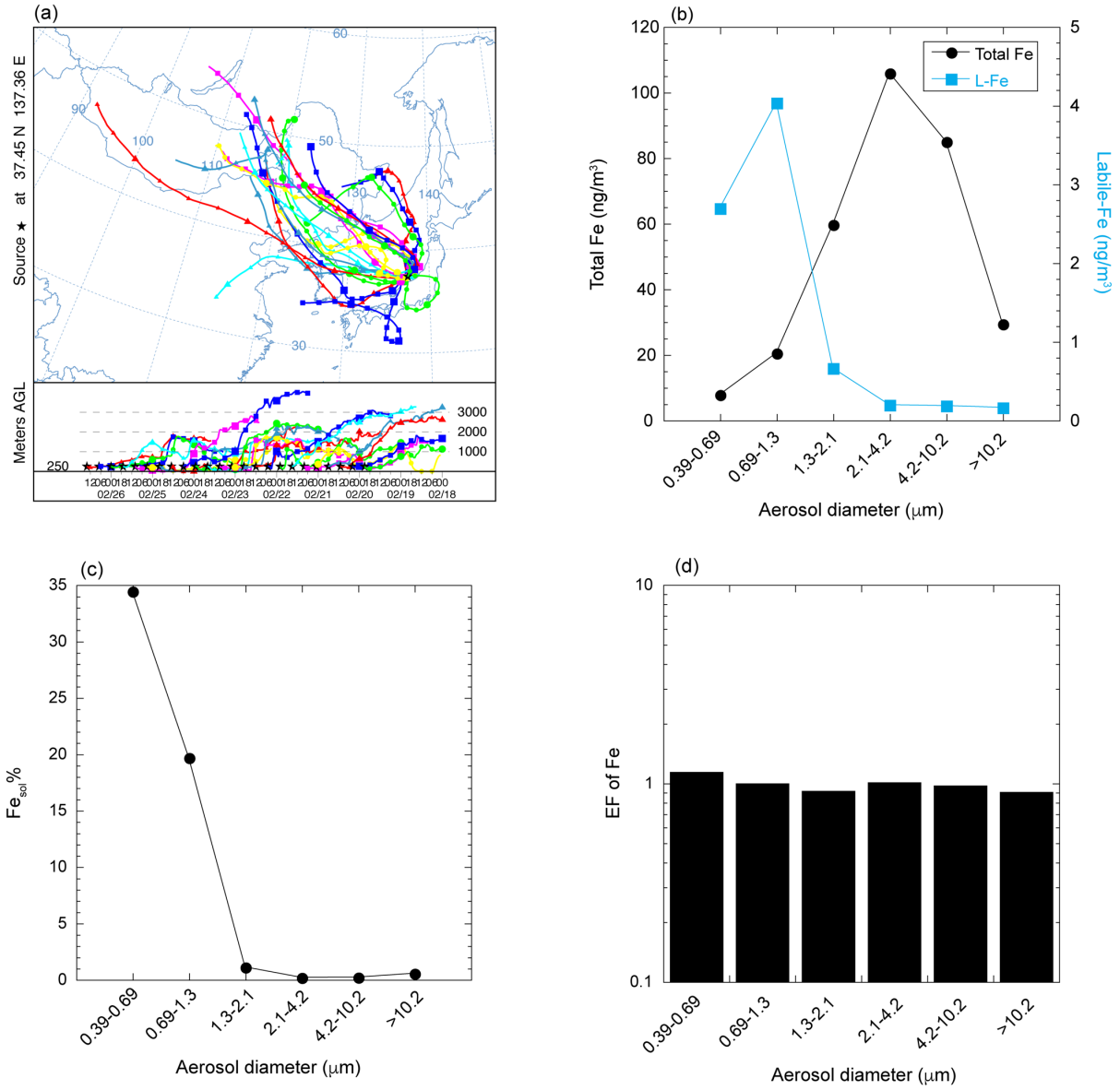

Figure S6: (a) backward trajectories, (b) total and labile Fe concentrations, (c) Fe_{sol}%, and (d) EF of Fe for the size-fractionated aerosol sample collecting in NOTOGRO. The backward trajectory was calculated by NOAA HYSPLIT (Stein et al., 2015).

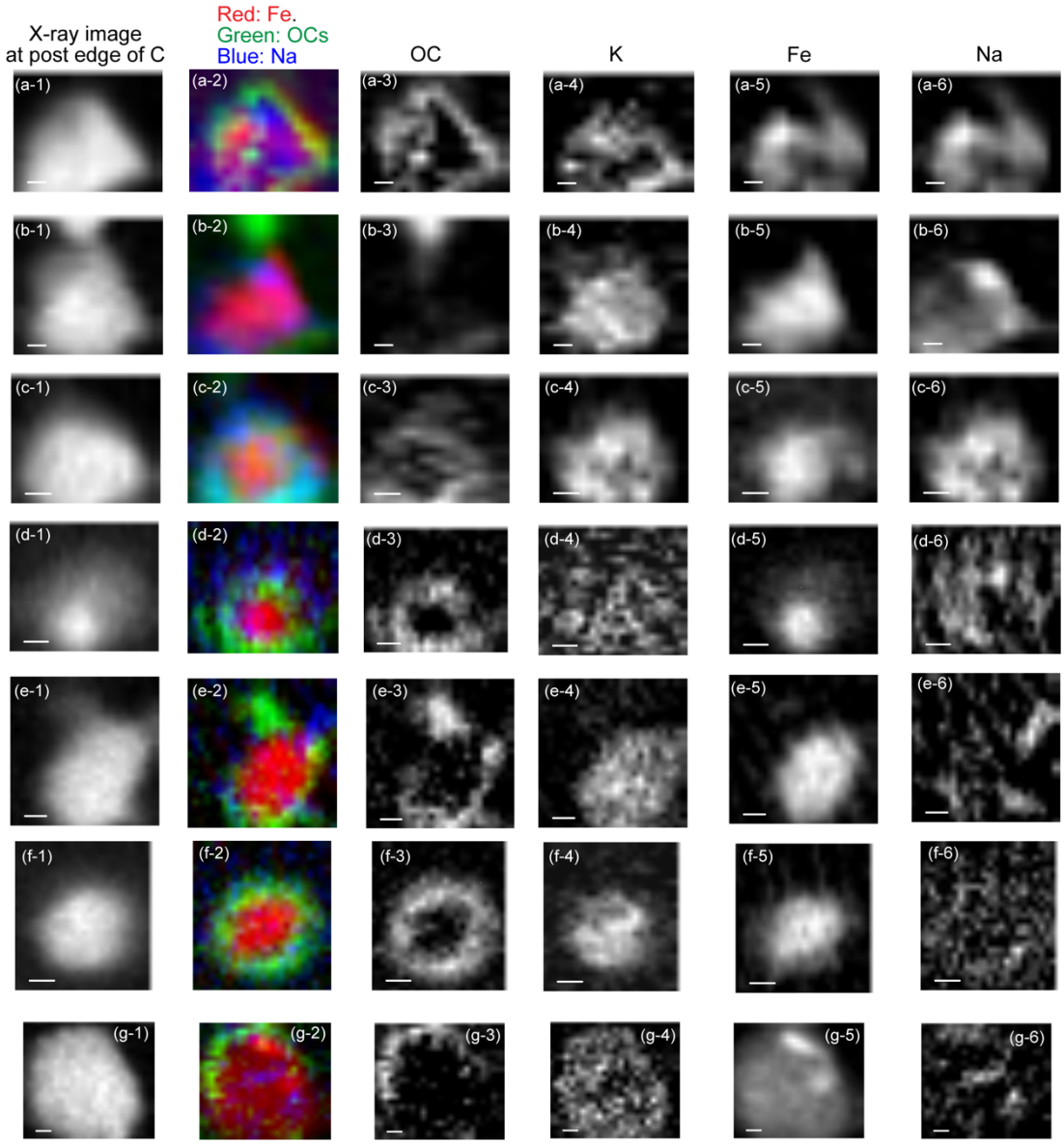

Figure S7: (a-1 to g-1) X-ray image of phyllosilicate particles in S6-WPO2, (a-2 to g-2) RGB composite of Fe (red), carboxylates (green) and Na (blue), (a-3 to g-3) distribution of OCs, (a-4 to g-4) distribution of potassium (K), (a-5 to g-5) distribution of Fe, and (a-6 to g-6) distribution of Na.

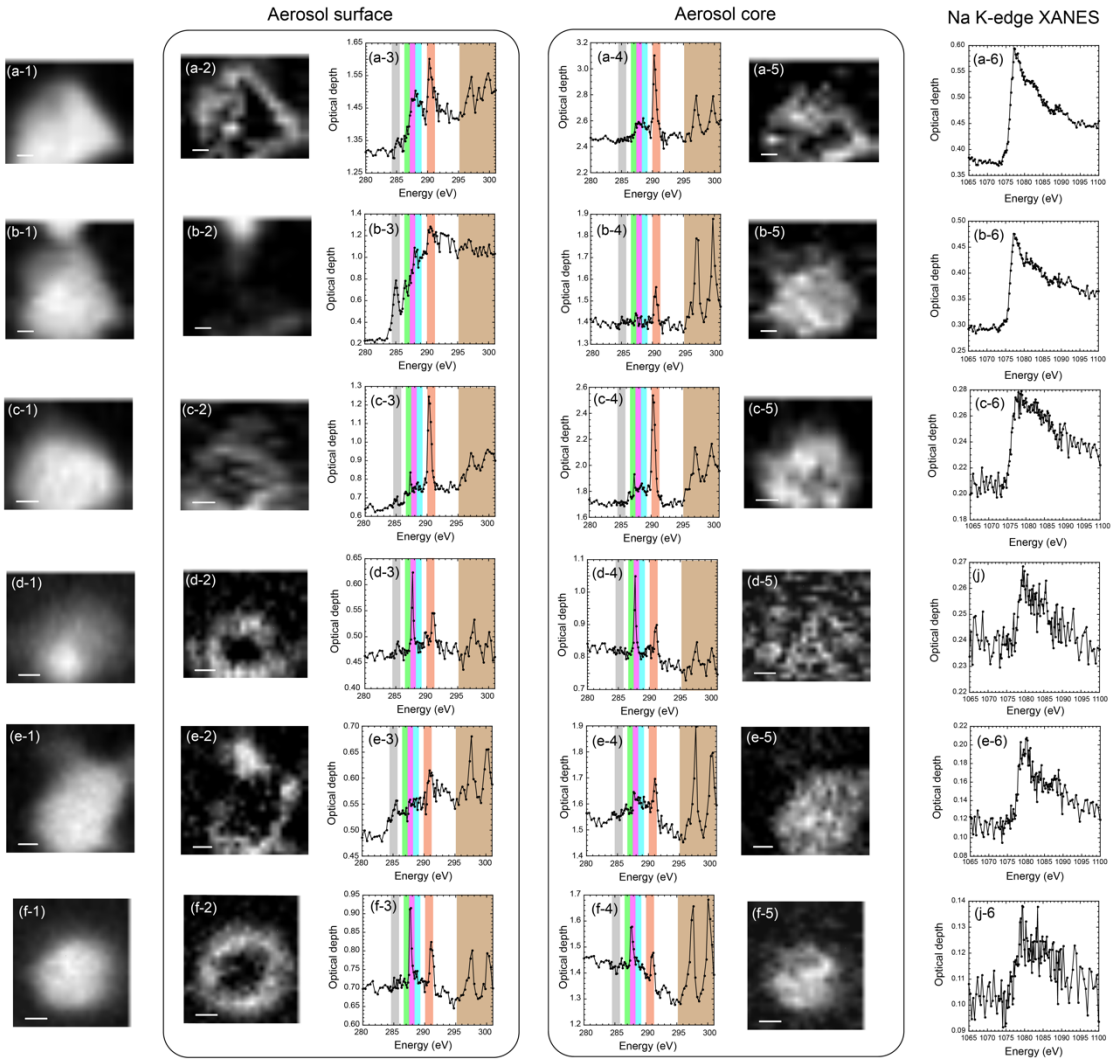

Figure S8: (a-1 to f-1) X-ray image of phyllosilicate particles of S6-WPO2, (a-2 to f-2) distribution of OCs, (a-3 to e-3 and a-4 to f-4) Carbon K-edge and potassium L-edge XANES spectra on the aerosol surface and in the aerosol core, respectively. Gray, light green, pink, light blue, orange, and brown regions show peak position of aromatic C, ketonic C, aliphatic C, carboxylates, carbonate, and potassium, respectively. (a-5 to e-5) distribution of potassium (K). (d) Na K-edge XANES spectra on the aerosol surface.

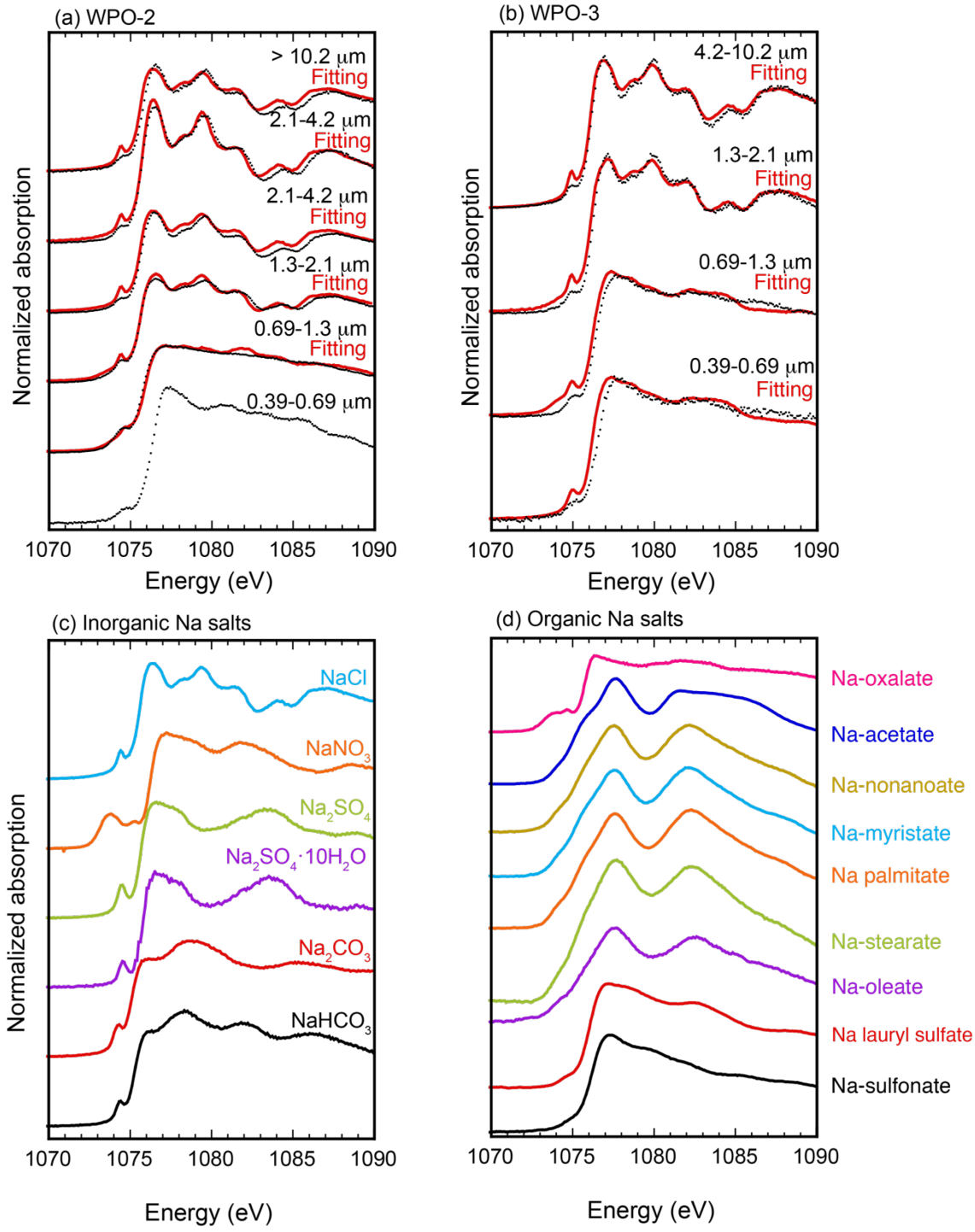

Figure S9: Na K-edge XANES spectra in size-fractionated aerosol samples collected in (a)WPO2 and (b) WPO3. The XANES spectra of reference materials of inorganic and organic Na salts are shown in panels (c) and (d), respectively.

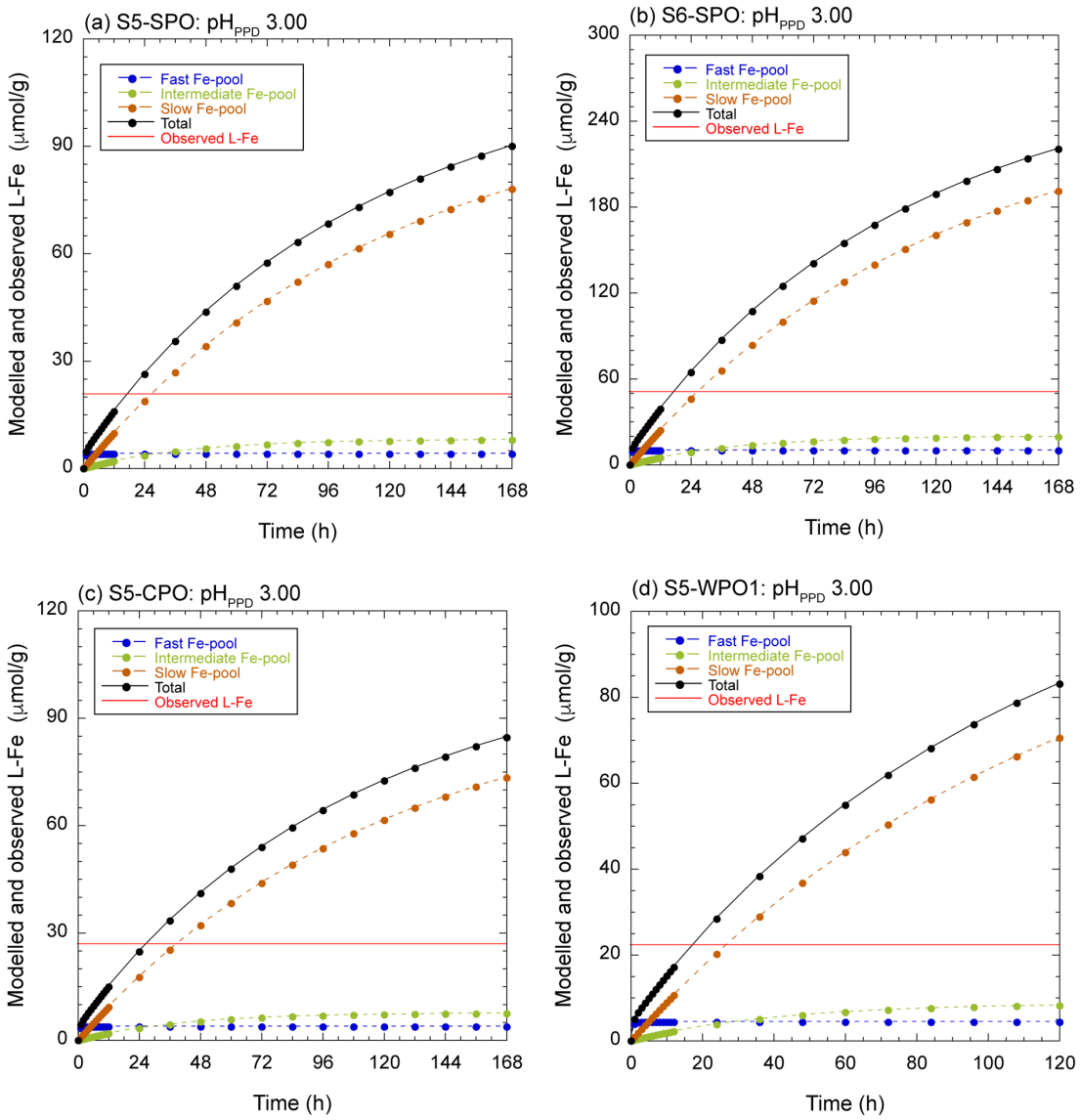

Figure S10: Dissolution curves for $PM_{1.3}$ with negative $[H^+]_{mineral}$: (a0 S5-SPO, (b) S6-SPO, (c) S5-CPO, and (d) S5-WPO1. The modeled L-Fe concentrations reached at the observed L-Fe concentration within 24 hours, even if pH_{PPD} was set 3.0. This result means that Fe-bearing particles were not acidified to solubilize Fe.

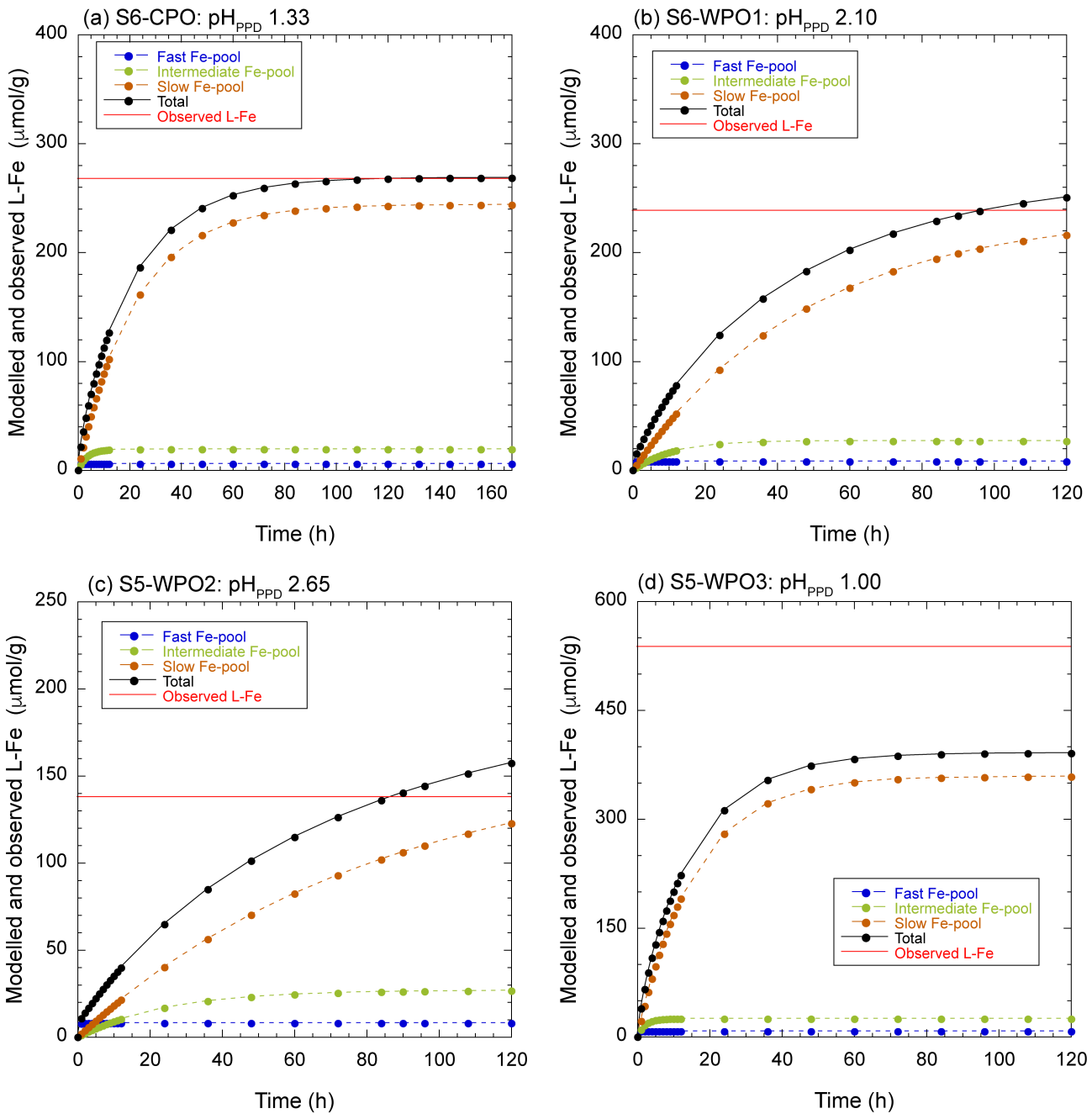

Figure S11: Dissolution curve of $PM_{1.3}$ with positive $[H^+]_{mineral}$; (a)S6-CPO, (b)S6-WPO1, (c) S5-WPO2, and (d) S5-WPO3. The observed L-Fe concentration in S6-WPO2 could not account for Fe dissolution at pH, indicating that Fe-bearing particles in the fractions underwent more acidic conditions.

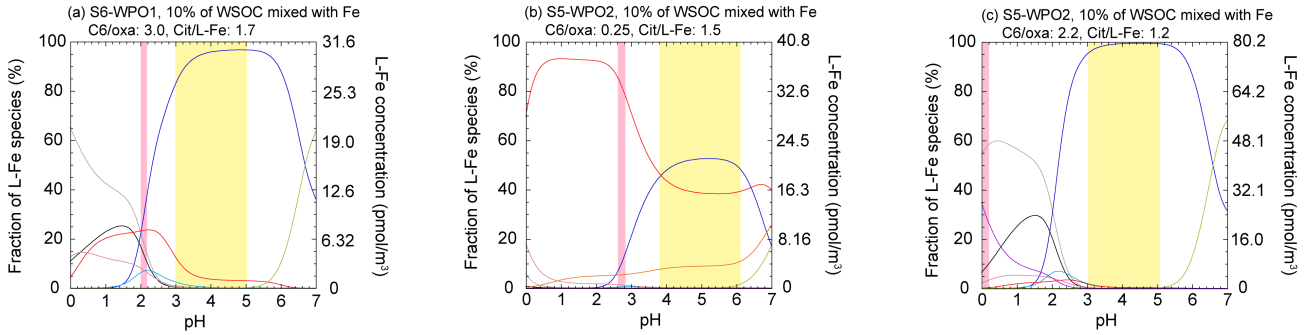

Figure S12: The pH dependences of Fe species in ALW calculated by GWB: (a) S6-WPO1, (b) S5-WPO2, and (c) S5-WPO3. The Citrate/L-Fe (Cit/L-Fe) ratio was estimated with assumption that 10% of WSOC in the fraction was mixed with Fe-bearing particles.

Table S1. Sampling information of the size-fractionated aerosols used in this study.

	Start			End			
	Time, Date (GMT)	Latitude	Longitude	Time, Date (GMT)	Latitude	Longitude	Total flow (m^3)
SPO	4:39, Jan. 10	49.39º S	170.00º W	11:40, Jan. 14	32.37º S	170.00º W	2256.1
CPO	20:41, Jan. 27	29.57º S	170.00º W	1:25, Feb. 1	15.07º S	170.00º W	1923.2
WPO1	5:35, Feb. 16	9.11º N	159.18º E	20:21, Feb. 18	12.42º N	143.36º E	1739.5
WPO2	19:29, Feb. 19	13.34º N	144.02º E	19:29, Feb. 21	21.25º N	144.03º E	1215.6
WPO3	9:59, Feb. 22	21.46º N	143.58º E	10:42, Feb. 24	32.07º N	140.47º E	973.0

Table S2. EF of Fe and Co in NIST standard reference materials (SRM) of coal and coal fly ashes.

	Fe	Co	
SRM®1632d	1.20	12.4	Coal
SRM®1635a	0.664	12.1	Coal
SRM®1633c	1.15	10.6	Coal fly ash
SRM®2689	1.05	12.2	Coal fly ash
SRM®2690	0.423	5.06	Coal fly ash

Thermodynamic data: Stability constants (log K) of main species in this study (only show 25ºC).

	Species	Reaction	Log K
		Fe species	
1.	$FeOH^+$	$Fe^{2+} + H_2O \rightarrow FeOH^+$	9.40
2.	$FeOH^{2+}$	$Fe^{3+} + H_2O \rightarrow FeOH^{2+}$	2.02
3.	$Fe(OH)_2$ (aq)	$Fe^{2+} + 2H_2O \rightarrow Fe(OH)_2$ (aq) $+ 2H^+$	20.5
4.	$Fe(OH)_2^+$	$Fe^{3+} + 2H_2O \rightarrow Fe(OH)_2^+ + 2H^+$	5.75
5.	$Fe(OH)_3^-$	$Fe^{2+} + 3H_2O \rightarrow Fe(OH)_3^-$ (aq) $+ 3H^+$	31.0
6.	$Fe(OH)_3$ (aq)	$Fe^{3+} + 3H_2O \rightarrow Fe(OH)_3^+ + 3H^+$	15.0
7.	$Fe(OH)_4^-$	$Fe^{3+} + 4H_2O \rightarrow Fe(OH)_4^- + 4H^+$	22.7
9.	$Fe_2(OH)_2^{4+}$	$2Fe^{3+} + 2H^+ + 2H_2O \rightarrow Fe_2(OH)_2^{4+}$	2.89
9.	Fe-$(oxalate)_2^-$	$Fe^{3+} + 2\cdot Oxalate^{2-} \rightarrow$ Fe-$(oxalate)_2^-$	15.5
10.	Fe-$(oxalate)_2^{2-}$	$Fe^{2+} + 2\cdot Oxalate^{2-} \rightarrow$ Fe-$(oxalate)_2^{2-}$	5.90
11.	Fe-$(oxalate)_3^{3-}$	$Fe^{3+} + 3\cdot Oxalate^{2-} \rightarrow$ Fe-$(oxalate)_3^{3-}$	19.8
12.	Fe-oxalate (aq)	$Fe^{2+} + Oxalate^{2-} \rightarrow$ Fe-oxalate (aq)	3.97
13.	Fe-$oxalate^+$	$Fe^{3+} + Oxalate^{2-} \rightarrow$ Fe-$oxalate^+$	9.15
14.	Fe-$citrate^-$	$Fe^{2+} + Citrate^{3-} \rightarrow$ Fe-$citrate^-$	5.89
15.	Fe-citrate (aq)	$Fe^{3+} + Citrate^{3-} \rightarrow$ Fe-citrate (aq)	13.1
16.	FeH-citrate (aq)	$Fe^{2+} + H^+ + Citrate^{3-} \rightarrow$ FeH-citrate (aq)	10.2
17.	FeH-$citrate^+$	$Fe^{3+} + H^+ + Citrate^{3-} \rightarrow$ FeH-$citrate^+$	10.2
18.	Fe(OH)-$citrate^-$	$Fe^{3+} + Citrate^{3-} + H_2O \rightarrow$ Fe(OH)-$citrate^-$	1.79
19.	$FeSO_4$ (aq)	$Fe^{2+} + SO_4^{2-} \rightarrow FeSO_4$ (aq)	2.39
20.	$FeSO_4^+$	$Fe^{3+} + SO_4^{2-} \rightarrow FeSO_4^+$	4.25
21.	$Fe(SO_4)_2^-$	$Fe^{3+} + 2SO_4^{2-} \rightarrow Fe(SO_4)_2^-$	5.38
22.	$FeCl^+$	$Fe^{2+} + Cl^- \rightarrow FeCl^+$	0.200
23.	$FeCl^{2+}$	$Fe^{3+} + Cl^- \rightarrow FeCl^{2+}$	1.48
		Al species	
24.	$AlOH^{2+}$	$Al^{3+} + H_2O \rightarrow AlOH^{2+} + H^+$	5.00
25.	$Al(OH)_2^+$	$Al^{3+} + 2H_2O \rightarrow Al(OH)_2^+ + 2H^+$	10.3
26.	$Al(OH)_3$ (aq)	$Al^{3+} + 3H_2O \rightarrow Al(OH)_3$ (aq) $+ 3H^+$	16.7

Thermodynamic data: Continued.

	Species	Reaction	Log K
27.	$Al(OH)_4^-$	$Al^{3+} + 4H_2O \rightarrow Al(OH)_4^- 4H^+$	23.0
28.	$AlSO_4^+$	$Al^{3+} + SO_4^{2-} \rightarrow AlSO_4^+$	3.81
29.	$Al(SO_4)_2^-$	$Al^{3+} + 2SO_4^{2-} \rightarrow Al(SO_4)_2^-$	5.58
30.	Al-oxalate$^+$	$Al^{3+} + Oxalate^{2-} \rightarrow$ Al-oxalate$^-$	7.73
31.	Al-$(oxalate)_2^-$	$Al^{3+} + 2{\cdot}Oxalate^{2-} \rightarrow$ Al-$(oxalate)_2^-$	13.4
32.	Al-$(oxalate)_3^-$	$Al^{3+} + 3{\cdot}Oxalate^{2-} \rightarrow$ Al-$(oxalate)_3^{3-}$	17.1
33.	AlOH-oxalate (aq)	$Al^{3+} + Oxalate^{2-} + H_2O \rightarrow$ AlOH-oxalate (aq)	2.57
34.	Al-citrate (aq)	$Al^{3+} + Citrate^{3-} \rightarrow$ Al-citrate (aq)	9.98
35.	Al-$(citrate)_2^{3-}$	$Al^{3+} + 2{\cdot}Citrate^{3-} \rightarrow$ Al-$(citrate)_2^{3-}$ (aq)	14.8
36.	AlH-citrate$^+$	$Al^{3+} + Citrate^{3-} + H^+ \rightarrow$ AlH-citrate$^+$	12.9
37.	$AlCl^{2+}$	$Al^{3+} + Cl^- \rightarrow AlCl^{2+}$	0.390
		Cu species	
38.	$CuOH^+$	$Cu^{2+} + H_2O \rightarrow CuOH^+ + H^+$	7.45
39.	$Cu(OH)_2$ (aq)	$Cu^{2+} + 2H_2O \rightarrow Cu(OH)_2$ (aq) $+ H^+$	16.23
40.	$Cu(OH)_3^-$	$Cu^{2+} + 3H_2O \rightarrow Cu(OH)_3^- + 2H^+$	26.6
41.	$Cu(OH)_4^{2-}$	$Cu^{2+} + 4H_2O \rightarrow Cu(OH)_4^{2-} + 3H^+$	39.7
42.	$CuSO_4$ (aq)	$Cu^{2+} + SO^{2-} \rightarrow CuSO_4$ (aq)	2.36
43.	Cu-oxalate (aq)	$Cu^{2+} + oxalate^{2-} \rightarrow$ Cu-oxalate (aq)	5.72
44.	Cu-$(oxalate)_2^{2-}$	$Cu^{2+} + 2{\cdot}oxalate^{2-} \rightarrow$ Cu-$(oxalate)_2^{2-}$	10.2
45.	Cu-citrate$^-$	$Cu^{2+} + citrate^{3-} \rightarrow$ Cu-citrate$^-$	7.57
46.	Cu-$(citrate)_2^{3-}$	$Cu^{2+} + 2{\cdot}citrate^{3-} \rightarrow$ Cu-$(citrate^-)_2^{3-}$	8.90
47.	Cu_2-$(citrate)_2^{2-}$	$2Cu^{2+} + 2{\cdot}citrate^{3-} \rightarrow Cu_2$-$(citrate)_2^{2-}$	16.9
48.	CuCl (aq)	$Cu^+ + Cl^- \rightarrow$ CuCl (aq)	3.10
49.	$CuCl^+$	$Cu^{2+} + Cl^- \rightarrow CuCl^+$	0.300
50.	$CuCl_2^-$	$Cu^+ + 2Cl^- \rightarrow CuCl_2^-$	5.42
51.	$CuCl_2$ (aq)	$Cu^{2+} + 2Cl^- \rightarrow CuCl_2$ (aq)	0.260
52.	$CuCl_3^{2-}$	$Cu^+ + 3Cl^- \rightarrow CuCl_3^{2-}$	2.29
53.	$CuCl_3^-$	$Cu^{2+} + 3Cl^- \rightarrow CuCl_3^-$	4.75
54.	$CuCl_4^{2-}$	$Cu^{2+} + 4Cl^- \rightarrow CuCl_4^{2-}$	-4.59

Thermodynamic data: Continued.

	Species	Reaction	Log K
55.	$CuNH_3^{2+}$	$Cu^{2+} + NH_4^+ \rightarrow CuNH_3^{2+} + H^+$	5.22
56.	$Cu(NH_3)_2^+$	$Cu^+ + 2NH_4^+ \rightarrow Cu(NH_3)_2^+ + 2H^+$	0.680
57.	$Cu(NH_3)_2^{2+}$	$Cu^{2+} + 2NH_4^+ \rightarrow Cu(NH_3)^{2+} + 2H^+$	11.1
58.	$Cu(NH_3)_3^{2+}$	$Cu^{2+} + 3NH_4^+ \rightarrow Cu(NH_3)^{2+} + 3H^+$	17.5
59.	$Cu(NH_3)_4^{2+}$	$Cu^{2+} + 4NH_4^+ \rightarrow Cu(NH_4)^{2+} + 4H^+$	24.7
		H species	
60.	H-oxalate$^-$	$H^+ + oxalate^{2-} \rightarrow$ H-oxalate$^-$	4.27
61.	H_2-oxalate (aq)	$2H^+ + oxalate^{2-} \rightarrow H_2$-oxalate (aq)	5.52
62.	H-citrate^{2-}	$H^+ + citrate^{3-} \rightarrow$ H-citrate^{2-}	6.40
63.	H_2-citrate$^-$	$2H^+ + citrate^{3-} \rightarrow H_2$-citrate$^-$	11.2
64.	H_3-citrate (aq)	$3H^+ + citrate^{3-} \rightarrow H_3$-citrate (aq)	14.3
		Other species	
65.	$NH_4SO_4^-$	$NH_4^+ + SO_4^{2-} \rightarrow NH_4SO_4^-$	1.03
66.	NH_4-oxalate$^-$	$NH_4^+ + oxalate^{2-} \rightarrow NH_4$-oxalate$^-$	0.900
67.	NaCl(aq)	$Na^+ + Cl^- \rightarrow$ NaCl (aq)	0.300
68.	$NaNO_3$ (aq)	$Na^+ + NO_3^- \rightarrow NaNO_3$ (aq)	0.550
69.	$NaSO_4^-$	$Na^+ + SO_4^{2-} \rightarrow NaSO_4^-$	0.740
70.	Na-oxalate$^-$	$Na^+ + oxalate^{2-} \rightarrow$ Na-oxalate$^-$	0.900
71.	Na-citrate^{2-}	$Na^+ + citrate^{3-} \rightarrow$ Na-citrate^{2-}	1.39
72.	KCl (aq)	$K^+ + Cl^- \rightarrow$ KCl (aq)	-0.300
73.	KNO_3 (aq)	$K^+ + NO_3^- \rightarrow KNO_3$ (aq)	-0.190
74.	KSO_4^-	$K^+ + SO_4^{2-} \rightarrow KSO_4^-$	0.847
75.	K-oxalate$^-$	$K^+ + oxalate^{2-} \rightarrow$ K-oxalate$^-$	0.800
76.	K-citrate^{2-}	$K^+ + citrate^{2-} \rightarrow$ K-citrate^{2-}	1.10
77.	$MgCl^+$	$Mg^{2+} + Cl^- \rightarrow MgCl^+$	0.600
78.	$MgSO_4$ (aq)	$Mg^{2+} + SO_4^{2-} \rightarrow MgSO_4$ (aq)	2.26
79.	Mg-oxalate (aq)	$Mg^{2+} + oxalate^{2-} \rightarrow$ Mg-oxalate (aq)	3.62
80.	Mg-citrate$^-$	$Mg^{2+} + citrate^{3-} \rightarrow$ Mg-citrate$^-$	4.89
81.	MgH-citrate (aq)	$Mg^{2+} + citrate^{3-} + H^+ \rightarrow$ MgH-citrate (aq)	8.91

Thermodynamic data: Continued.

	Species	Reaction	Log K
82.	MgH_2-citrate$^+$	$Mg^{2+} + citrate^{3-} + 2H^+ \rightarrow MgH_2$-citrate$^+$	12.3
83.	$CaCl^+$	$Ca^{2+} + Cl^- \rightarrow CaCl^+$	0.400
83.	$CaCl^+$	$Ca^{2+} + Cl^- \rightarrow CaCl^+$	0.400
84.	$CaNO_3^+$	$Ca^{2+} + NO_3^- \rightarrow CaNO_3^+$	0.500
85.	$CaSO_4$ (aq)	$Ca^{2+} + SO_4^{2-} \rightarrow CaSO_4$ (aq)	2.36
86.	Ca-oxalate (aq)	$Ca^{2+} + oxalate^{2-} \rightarrow$ Ca-oxalate (aq)	3.19
87.	Ca-citrate$^-$	$Ca^{2+} + citrate^{3-} \rightarrow$ Ca-citrate$^-$	4.87
88.	CaH-citrate (aq)	$Ca^{2+} + citrate^{3-} + H^+ \rightarrow$ CaH-citrate (aq)	9.26
89.	CaH_2-citrate$^+$	$Ca^{2+} + citrate^{3-} + 2H^+ \rightarrow CaH_2$-citrate$^+$	12.6